IEEE Photonics Journal
An IEEE Photonics Society Publication

Open Access

Experimental Investigation of Large Time–Bandwidth Product Photonic Hilbert Transformer Based on Compact Bragg Grating

Volume 8, Number 4, August 2016

B. Liu
C. Sima
W. Yang
B. Cai
D. Liu
Y. Yu
J. Gates
M. Zervas
P. Smith

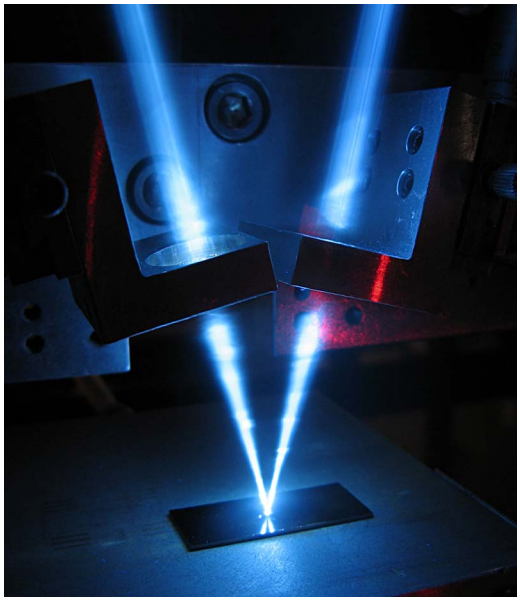

DOI: 10.1109/JPHOT.2016.2590941
1943-0655

IEEE photonics SOCIETY

IEEE

Experimental Investigation of Large Time–Bandwidth Product Photonic Hilbert Transformer Based on Compact Bragg Grating

B. Liu,[1] C. Sima,[1,2] W. Yang,[1] B. Cai,[1] D. Liu,[1] Y. Yu,[2] J. Gates,[3] M. Zervas,[3] and P. Smith[3]

[1]Next Generation Internet Access National Engineering Laboratory, Huazhong University of Science and Technology, Wuhan 430074, China
[2]Wuhan National Laboratory for Optoelectronics, Huazhong University of Science and Technology, Wuhan 430074, China
[3]Optoelectronics Research Centre, University of Southampton, Southampton SO17 1BJ, U.K.

DOI: 10.1109/JPHOT.2016.2590941

Manuscript received May 24, 2016; revised July 6, 2016; accepted July 9, 2016. Date of publication July 13, 2016; date of current version August 8, 2016. This work was supported by the National Natural Science Foundation of China under Grant 61404056 and Grant 61475050. Corresponding author: C. Sima (e-mail: smct@hust.edu.cn).

Abstract: We propose and experimentally demonstrate an integrated photonic Hilbert transformer (PHT) with substantial time bandwidth product (TBP). Due to the current substrate material and fabrication technique, PHT devices find it challenging to achieve ultrawide operative bandwidth while maintaining the minimum bandwidth level presented as the narrow central notch in frequency response. This implies that the TBP value is restricted. Here, we investigate the synthesized refractive index profile in compact Bragg grating design for theoretical simulation and the linearity-enhanced direct UV grating writing fabrication for experimental implementation. The fabricated device could process microwave photonic signals as Hilbert transformation between 50 GHz and 3 THz, with the TBP above 60, which is the largest experimental data to the best of our knowledge. This technique allows the PHT with improved spectral performance to be suitable for analog all-optical signal processing.

Index Terms: Ultrafast devices, gratings, waveguide devices, microwave photonics signal processing.

1. Introduction

In microwave photonics, the time-bandwidth product (TBP) is a principle figure of merit, defined as the ratio between the processing time windows to the fastest time feature that can be accurately processed [1], [2]. It is the product of frequency bandwidth and pulse duration of a signal, which indicates occupation of the signal in both time and frequency domain. Microwave implementation with large TBP has been widely employed, for instance, to improve the range solutions in modern radar systems, microwave computed technology, and spread-spectral communication [3]. With the development of analog optical signal processing technology, the optical signal processing with advanced TBP is required.

The Photonic Hilbert transformer (PHT) has been extensively used in various fields, e.g., single sideband filtering, microwave photonic signal generation, image processing, and so on [4]–[10]. In the implementation of the Hilbert transform, the TBP of the Hilbert transform devices is the product of output signal with unit input impulse, which also implies the capability of generating signals with large TBP ratio. It is reported that the duration of impulse response is approximately equal to the minimum bandwidth of the frequency spectrum [5]. Hence, the TBP of the Hilbert transformer could be derived to be a ratio of maximum bandwidth and minimum bandwidth in frequency domain. Using long period gratings [11], the TBP was also referred and related to grating lengths by measuring estimated maximum and minimum operating bandwidths for different truncation windows; experiment data of this technique are to be exhibited.

In experimental demonstrations [6]–[10], PHT devices are challenging to achieve ultra-wide operative bandwidth while maintaining the narrow central notch in the frequency response. The TBP was somewhat restricted, due to either fabrication techniques (e.g., phase-mask scanning techniques) or substrate materials (e.g., limited refractive index contrast). Recently, waveguide PHTs with TBP approaching 26 were realized based on phase shifted silicon gratings [9], with advantages of small footprint and complementary metal-oxide semiconductor (CMOS) platform compatibility.

Here, we propose the TBP to evaluate the spectral quality particularly operative bandwidth features in PHT, theoretically analyze the synthesized refractive index profile in compact Bragg grating design for simulation, and develop the linearity-enhancement module in the conventional direct UV writing technique for fabrication. Fabricated devices with planar geometry could process microwave photonic signals as Hilbert transformation between 50 GHz and 3 THz and maintain constant amplitude, which implies the TBP over 60: virtually ten folds larger than those fiber-based experiments. With benefits of an integrated structure and fiber compatibility, this technique has potential in enabling direct and ultra-wide analog optical signal processing.

2. Theory and Principles

The Fourier transform of the kernel of the Hilbert transform is [4]

$$H(\omega) = -j\mathrm{sgn}(\omega) \tag{1}$$

where ω is the angular frequency, and $\mathrm{sgn}(\omega)$ is the sign function (which is $+1$ for $\omega > 0$, 0 for $\omega = 0$ and 1 for $\omega < 0$). However, this PHT is not realizable in practice, because of i) its frequency infinite bandwidth, ii) infinite amplitude of the corresponding impulse response at $t = 0$, and iii) infinite duration of the corresponding impulse response. For a physically realizable PHT, we limited the frequency bandwidth and the corresponding impulse duration to get impulse response $h(t)$ by Fourier transform. Through the space-frequency-time mapping technique [5], the grating refractive index profile Δn is

$$\Delta n(z) \propto \sin^2[\pi n_{\mathrm{eff}} \Delta f(z - z_0)/c]/(z - z_0) \tag{2}$$

where n_{eff} is the grating effective refractive index, z is the grating length, and z_0 is the zero-crossing point in the apodization function. This refractive index profile allows the straightforward design and fabrication of Bragg gratings.

To characterize the spectral quality of the PHTs, the TBP is employed, which accounts for the product of the frequency bandwidth of PHT and the pulse width of impulse response of Hilbert transform. Asghari and Azana have analyzed that the duration of impulse response is approximately equal to the minimum bandwidth of the frequency spectrum [5]; hence, the TBP is virtually equivalent to the ratio of the maximum bandwidth to the minimum bandwidth of Hilbert transform. It is also calculated at 3 dB decay in the power spectral responses [11]. The derivation is shown as

$$\mathrm{TBP} = \Delta f \times \Delta t \approx \Delta f \times 1/f_{\mathrm{min}} = \frac{f_{\mathrm{max}}}{f_{\mathrm{min}}}. \tag{3}$$

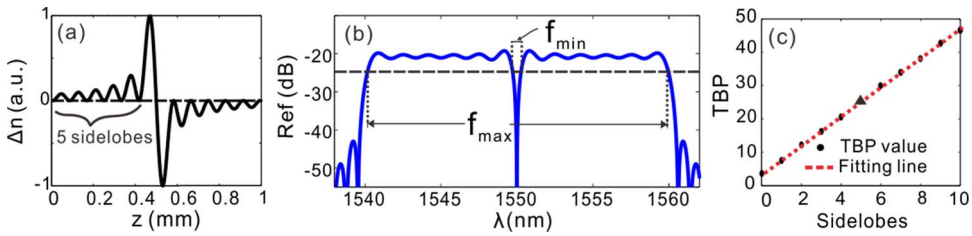

Fig. 1. Simulation data. (a) Grating refractive index profile for PHTs. (b) Amplitude response of PHTs showing the maximum (f_{max}) and minimum (f_{min}) operative bandwidths. (c) Relationship between the number of sidelobes and the calculated time–bandwidth product.

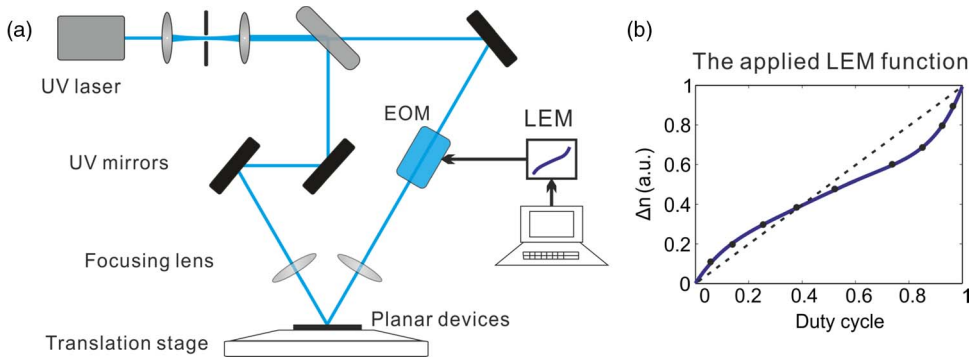

Fig. 2. (a) Crossed beam direct UV grating writing scheme: EOM—electrooptical modulator; LEM—linearity enhancement module. (b) Synthesized linearity enhancement function applied to the grating fabrication.

3. Experimental Details

The device output for the proposed structure was modeled using the transfer matrix method. The following parameters were used: grating length $z = 1$ mm, $n_{eff} = 1.45$, and the max grating refractive index modulation depth $\Delta n = 8 \times 10^{-4}$.

Fig. 1(a) presents the grating refractive index profile with 2.5 THz bandwidth, including a main lobe and five sidelobes. Fig. 1(b) illustrates the reflectivity spectrum of the proposed Bragg grating, and it indicates the TBP is approx. 26 ($f_{max} = 2.43$ THz, $f_{min} = 95$ GHz), while employing the grating refractive index profile with five sidelobes shown in Fig. 1(a). Fig. 1(c) shows the relationship between the number of sidelobes in the grating refractive index profile and the device TBP ratio, and presents an almost linear relationship. The triangle point located in Fig. 1(c) presents the scenario of implementing the refractive index profile in Fig. 1(a). Modeling data also implies that the added number of apodization sidelobes leads to the increasing TBP ratio and contributes to the smoother and top-flatter amplitude response.

The proposed devices were fabricated using the DGW technique with phase modulation [12], as shown in Fig. 2(a). The DGW method involves two crossed laser beams into a photosensitive core of a planar waveguide, which promises the focused spot diameter around 6 um. Phase modulation is applied to one arm of the interferometer via the EOM, and this controls the relative position of the interference fringe pattern. Constant translation of the sample and modulation of the fringe pattern position defines the channel waveguide and simultaneously allows creation of the grating structures. Fig. 2(b) shows the employed linearity enhancement module during the grating fabrication. With such high dimensional resolution, it is available to fabricate Bragg gratings with precious refractive index control in micrometers range, which is significant for the PHT devices. To achieve the substantial TBP as previously discussed, the sidelobes effect of grating refractive index profile and the compact grating structure were both considered.

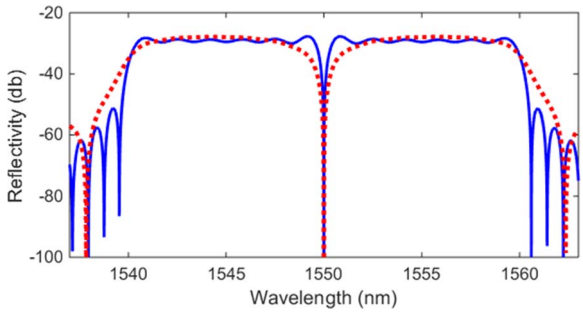

Fig. 3. Simulation of reflectivity in (red dotted line) nonlinear condition and (blue solid line) compensated linear condition.

According to the above analysis, it is crucial to maintain the designed shape of the grating refractive index profile, particularly the effect of the slight sidelobes variations located away from the grating central position. When applying the grating apodization in the conventional DGW technique or common phase mask scanning techniques, the refractive index is expected to change linearly with the control factor, e.g., duty cycle. Nevertheless, as a matter of fact, the relationship would not behave completely linearly, usually as nonlinearity. The nonlinearity is manifested by a lagging phenomenon at the beginning of the ultraviolet induced refractive index change and saturation phenomenon in the end probably due to the exhaust of photosensitive lattice in the core.

In most cases, this nonlinear effect is ignored since its slight effect on the grating spectrum. For instance, when employing Gaussian apodized gratings for optical filtering or optical sensing, the superposition of nonlinear effect and the designed Gaussian apodization curve still leads to a Gaussian-like refractive index profile and achieve Gaussian shape spectrum consequently. Notwithstanding, in this work the nonlinear phenomena has significant impact on the PHT spectra, evaluated as the TBP value to be considered thoroughly. We have previously attempted to explore the nonlinearity phenomena of the Δn_{ac} versus duty cycle in the DGW technique [13]. The synthesis process is applied for linear enhancement during device fabrication, shown in Fig. 2(b). By means of the linearity enhancement function, the relation between duty cycle and controlled refractive index is compensated for linearity. Comparison of the simulated reflectivity spectra in nonlinear (red dotted line) and compensated linear (blue solid line) condition are shown in Fig. 3. It is estimated the TBP value increases four times through the linearity enhancement.

The fabricated devices had three layers of silica deposited on a silicon substrate, and consisted of a thermal oxide layer (lower clad), core and an upper clad. The thickness of the core was about 8 μm, which ensured vertical single mode operation. The Bragg grating was 1 mm long which contains about 10 sidelobes in the refractive index profile, and Δn_{ac} is around 8×10^{-4}. We carried out corresponding experiments to measure the characteristics in both frequency domain and time domain.

Firstly, through a system that consists of an optical spectral analyzer, an optical circulator and a continuous laser resource, the frequency characteristics are straightly measured. Fig. 4(a) shows the measured reflectivity data of the fabricated devices with 2.5 THz (blue line) and 3 THz (red line) maximum bandwidths, and the insert illustrates below 50 GHz minimum operative bandwidths. Henceforth, PHT gratings with large TBP over 60 are demonstrated. Meanwhile, the PHT has a flattop amplitude response with about 2 dB ripples. The reflectivity of PHT is relatively below –20 dB as a result of the broaden bandwidth. The measurement system has limited dynamic range resulting in a noise floor of about –30 dB of the reflectivity measurement. As previously reported [12], the capability of ultra-accurate grating control (in nanometers precision) in the direct UV grating fabrication technique guarantees the phase response is to be with π phase shift in the central frequency. Lack of equipment for the direct optical phase

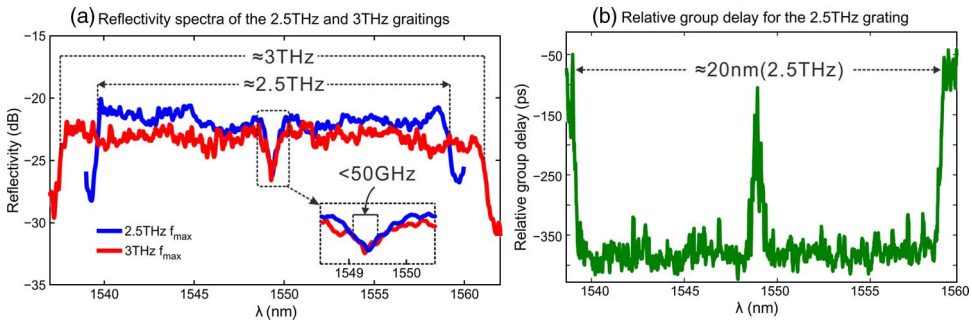

Fig. 4. (a) Measured reflectivity spectra of the fabricated PHT devices, with the insets showing operative bandwidth from below 50 GHz to 2.5 THz (blue) and 3 THz (red). (b) Measured relative group delay for the 2.5-THz grating.

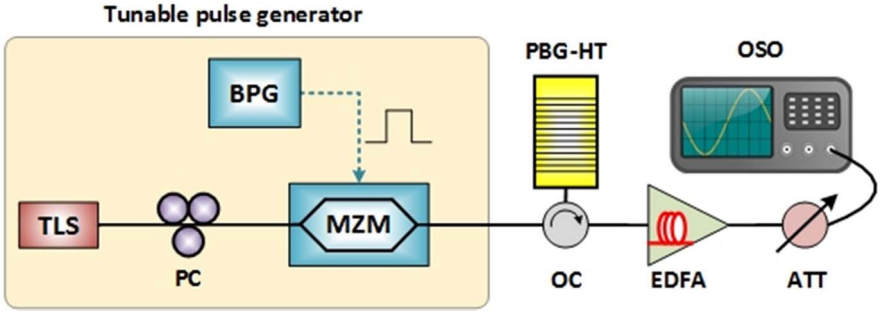

Fig. 5. Temporal measurement setup. TLS: tunable laser source; PC: phase controller; MZM: Mach–Zehnder modulator; BPG: bit pattern generator; EDFA: erbium-doped optical fiber amplifier; OC: optical circulator; PBG-HT: planar Bragg grating of Hilbert transform; ATT: attenuator; OSO: optical sampling oscilloscope.

measurement, the modulation phase-shift method was alternatively used to obtain relative group delay data, by comparing the change in phase of the received microwave waveform with the original modulated sinusoidal waveform using a vector network analyzer [13]. Fig. 4(b) shows the relative group delay for the 2.5 THz grating. The behavior of this phase shift is also verified by the following temporal impulse characterization.

Second, to obtain the device temporal impulse response, the following setup is utilized in the experiment, as shown in Fig. 5. The experimental configuration mainly consists of three parts: the pulse generator, the PHT grating, and the sampling oscilloscope. The pulse generator part is to generate Non-Return-To-Zero (NRZ) pulse which is frequency tunable and pulse-width tunable. In the pulse generation part, the polarization-controlled continuous wave light from the tunable laser source (TLS) is firstly modulated by the Mach–Zehnder modulator (MZM) with data from bit pattern generator (BPG). To obtain the NRZ pulse, the parameters and direct current bias should be carefully adjusted. Modulated by data with different width and repetitive rate, disparate NRZ pulse can be generated. To compensate the loss induced by the MZM and planar Bragg grating of Hilbert transform (PBG-HT), an erbium-doped optical fiber amplifier (EDFA) is employed. Temporal pulses with different FWHM can be obtained through changing the data from the BPG. Then, the repeated pulse generated by the generator part is sent to the PBG-HT. Subsequently, the output pulse of PHT is amplified by an EDFA compensating the loss induced by the PHT, and eventually sent to the optical sample oscilloscope for analysis.

Due to the current available microwave devices, the measured microwave frequency range is limited to tens of gigahertz. Thus, through the same process, we fabricated a similar PHT grating but with narrower operative range between 20 GHz and 800 GHz. An input NRZ pulse at around 40 Gbps with pulse width around 60 ps is generated and sent into the PHT grating. The output

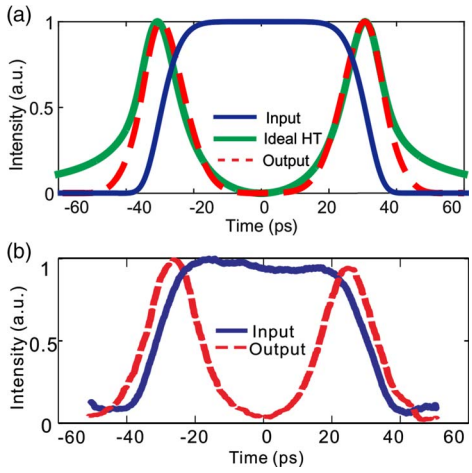

Fig. 6. (a) Simulation data for (blue solid line) input pulse, (red dashed line) output temporal waveform, and (green solid line) output from ideal Hilbert transform. (b) Experimental results for temporal PHT with (blue solid line) input pulse and (red dashed line) output temporal waveform.

data is collected by the optical sample oscilloscope. Fig. 6(a) shows the simulated data. A Hermite–Gaussian pulse is used to model the input NRZ pulse. The input pulse waveform (blue solid line) and the simulated output waveform (red dashed line) are both included in Fig. 6(a). For comparisons, we present the output waveforms with the same input pulse from ideal Hilbert transform (ideal HT, green solid line). It is observed that the output of PHT based on planar grating is basically matched with the output of the ideal HT, which is an infinite frequency response. The comparison of PHT and optical differential is discussed in the literature [14] and we shall present this discussion in future work. Fig. 6(b) shows the normalized experimental data of the input pulse (blue solid line) and the corresponding output Hilbert-transformed waveform (red dashed line). It is observed that, comparing the experimental output waveform and simulated data, the device performance is apparently consistent.

4. Conclusion

In conclusion, we have experimentally demonstrated a spectral quality improved large time-bandwidth product PHT, using a compact Bragg grating structure. The proposed grating devices are fabricated via the linear-enhanced direct UV grating writing technique. The sidelobes in the grating refractive index profile and the linear enhancement method in the fabrication process both contribute to the device TBP enlargement and spectral quality improvements including flatness and operating bandwidths. The TBP above 60 is achieved experimentally, with devices operating from 50 GHz to 3 THz. The temporal impulse responses are also analyzed for verification. This technique has prospects in precise handling and processing of ultra-broadband microwave photonic signals.

References

[1] A. Seeds and K. Williams, "Microwave photonics," *IEEE J. Lightw. Technol.*, vol. 24, no. 12, pp. 4628–4641, Dec. 2006.
[2] M. Ferrera *et al.,* "On-chip CMOS-compatible all-optical integrator," *Nature Commun.*, vol. 1, no. 3, pp. 605–629, 2010.
[3] C. Wang and J. Yao, "Large time–bandwidth product microwave arbitrary waveform generation using a spatially discrete chirped fiber Bragg grating," *IEEE J. Lightw. Technol.*, vol. 28, no. 11, pp. 1652–1660, Jun. 2010.
[4] A. D. Poularikas, *The Transforms and Applications Handbook*, 2nd ed. Boca Raton, FL, USA: CRC, 2000.
[5] M. H. Asghari and J. Azana, "All-optical Hilbert transformer based on a single phase-shifted fiber Bragg grating: Design and analysis," *Opt. Lett.*, vol. 34, no. 3, pp. 334–336, 2009.

[6] M. Li and J. Yao, "Experimental demonstration of a wideband photonic temporal Hilbert transformer based on a single Fiber Bragg grating," *IEEE Photon. Technol. Lett.*, vol. 22, no. 21, pp. 1559–1561, Nov. 2010.
[7] Z. Li, Y. Han, H. Chi, X. Zhang, and J. Yao, "A continuously tunable microwave fractional Hilbert transformer based on a nonuniformly spaced photonic microwave delay-line filter," *IEEE J. Lightw. Technol.*, vol. 30, no. 12, pp. 1948–1953, Jun. 2012.
[8] L. Zhuang *et al.,* "Novel microwave photonic fractional Hilbert transformer using a ring resonator-based optical all-pass filter," *Opt. Exp.*, vol. 20, pp. 26499–26510, 2012.
[9] M. Burla *et al.,* "Terahertz-bandwidth photonic fractional Hilbert transformer based on a phase-shifted waveguide Bragg grating on silicon," *Opt. Lett.*, vol. 39, pp. 6241–6244, 2014.
[10] W. Liu *et al.,* "A fully reconfigurable photonic integrated signal processor," *Nature Photon.*, vol. 10, pp. 190–195, 2016.
[11] R. Ashrafi and J. Azana, "Terahertz bandwidth all-optical Hilbert transformers based on long-period gratings," *Opt. Lett.*, vol. 37, pp. 2604–2607, 2012.
[12] C. Sima *et al.,* "Ultra-wide detuning planar Bragg grating fabrication technique based on direct UV grating writing with electro-optic phase modulation," *Opt. Exp.*, vol. 21, pp. 15747–15754, 2013.
[13] P. A. Williams, "Modulation phase-shift measurement of PMD using only four launched polarisation states: A new algorithm," *Electron. Lett.*, vol. 35, pp. 1578–1579, 1999.
[14] T. Yang *et al.,* "Experimental observation of optical differentiation and optical Hilbert transformation using a single SOI microdisk chip," *Sci. Rep.*, vol. 4, 2014, Art. no. 3960.